https://erjm.journals.ekb.eg
ISSN: 1110-1180

DOI: ---------

ERJ
Engineering Research Journal
Faculty of Engineering
Menoufia University

Thermal Properties Investigation of a Novel Phase Change Material Based on Nanocomposites of Paraffin Wax and Amorphous Nanosized TiO_2

Ragab A. Elsad*, Ahmed A. Atwa, Elsayed M. Farag, Shehab A. Mansour

Basic Engineering Science Department, Faculty of Eng. Menoufia University, Shebin El-Kom, Egypt
**(Corresponding author: ragab.elsad@gmail.com)*

ABSTRACT

Energy transmission and storage are vital in modern applications, especially for photovoltaic thermal (PV/T) applications. One of the significant advancements employed in these applications is phase change materials (PCMs), which offers improved thermophysical characteristics. In this regard, embedded Paraffin wax (PW) and amorphous TiO_2 (a-TiO_2) nanoparticles (NPs) were prepared. The sonochemical hydrolysis method is used to produce a-TiO_2 NPs. The embedded concentrations of a-TiO_2 NPs in PW in this study are 0, 0.05, 0.1, 0.15, 0.2, 0.25, 0.3, and 0.5 wt%. The morphological features of synthesized a-TiO_2 NPs as well as PW/a-TiO_2 nanocomposites (NCs) were examined by field emission scanning electron microscope (FE-SEM). Differential scanning calorimeter (DSC) investigations were used to determine the viability of these materials for thermal storage by evaluating the effects of various a-TiO_2 NP concentrations on the melting point (Tm), latent heat rate (SP), and latent heat of fusion (LH) of PW. PW/a-TiO_2 NCs had LH and SP values that are higher than those found in pure PW samples. SP value increased with TiO2 content up to 0.25 weight percent before declining with additional contents. While LH was improved with TiO2 up to 0.15 wt% content and subsequently dropped for additional contents. LH and SP values for PW/a-TiO2 NCs were significantly improved compared to pure PW samples by 19.1% and 298.6%, respectively.

Keywords: *Phase change materials; amorphous; TiO_2; NPs; latent heat rate (SP); latent heat of fusion (LH).*

1. Introduction

Solar energy is one of the most promising renewable energy sources. It is employed to generate thermal energy for usage in numerous industrial and home applications. The intermittent nature of solar energy makes it difficult to completely rely on it today; this leads to a discrepancy between the sun irradiation and the demand for thermal energy. As one of the most effective and environmentally friendly methods for storing solar energy, thermal energy storage (TES) systems are increasingly frequently utilized to correct the imbalance between solar irradiation and thermal energy demand [1]. Phase change materials (PCMs) are materials that release or absorb sufficient heat energy during their phase change to provide useable cooling or heat. The utilizing of PCMs in TES systems as functional materials has attracted researchers interest for their sensible heat (SH) and latent heat (LH) and for their thermal properties such as, melting temperature (Tm) within the temperature range required for the operation, suitable latent heat (LH) of melting, high thermal stability, and durability [2, 3]. Paraffin wax (PW) is one of the most important organic PCMs, which consists of a straight chain of hydrocarbons. It's widely used in TES systems nowadays due to its suitable thermal stability below 500 °C, lack of phase separation, availability, and low cost, but it has some drawbacks such as, low thermal conductivity and lower heat of melting when compared to inorganic PCMs [4-6]. To overcome these drawbacks, a lot of researchers have done their best to enhance the thermal properties of PW by adding inorganic nanoparticles (NPs) such as, TiO_2, ZnO, CuO and Al_2O_3. Tun-Ping Teng et al. [7], examined the thermal properties of PW with different NPs such as, TiO_2, Al_2O_3, ZnO and SiO_2. The results showed that TiO_2 has more effect on enhancing thermal storage characteristics and heat conduction performance of PW. Wang et al. [8], studied the effect of dispersing TiO_2 on PW. The results showed an enhancement in the thermal properties of the investigated TiO_2/PW nanocomposites (NCs) as their thermal conductivity was enhanced compared to pure PW. They reported that the thermal conductivity increased with the increase of TiO_2 NPs loading. Ho and Gao [9], examined the thermal properties of PW after dispersing Al_2O_3 NPs in PW. Their results showed that the dynamic viscosity and thermal conductivity of the investigated NCs was increased nonlinearly with increasing NPs mass fraction. Gunjo

DG et al. [10], studied numerically the enhancement of melting of PW with loading Cu, CuO and Al_2O_3 NPs. They reported that the addition of 5% from Cu, CuO and Al_2O_3 NPs in PW has enhanced the melting rate by 10, 2.25 and 3.46 times and the discharging rate by 8, 1.7 and 3 times respectively compared to pure PW.

There are many challenges in understanding the PW NCs behavior such as determining the suitable range of loaded NPs that is required to enhance the thermal properties of PW. This depends mainly on many factors for the loaded NPs such as, thermal properties, size, shape, structural phase and the introducing method in PW. Obviously, research works are needed to reach the optimum conditions of using PW NCs in TES systems.

2. Aim and Research Significance

Most of research works used crystalline TiO2 in the anatase phase as NPs, the present work studies the PW/amorphous TiO2 (a-TiO2) NCs thermal properties by loading a low range of a-TiO2 NP concentrations up to 0.5 wt% with different steps of concentration; 0, 0.05, 0.1, 0.15, 0.2, 0.25, 0.3 and 0.5 wt%. The a-TiO2 structural, optical and electronic properties are similar to crystalline TiO_2 properties in many respects and it's much closer to anatase phase of TiO_2, this opened the possibility of using a-TiO_2 NPs instead of crystalline TiO_2 NPs due to its low density, rough surface compared to crystalline TiO_2 and the reduced cost of synthesization at low temperature [11]. The effect of adding a-TiO_2 on thermal properties of PW was studied using non-isothermal differential scanning calorimetry (DSC) which determined the characteristic parameters of melting process for the investigated PW/a-TiO_2 NCs.

3. Experimental Details

3.1 Materials

PW/a-TiO_2 NCs were made using raw materials that did not undergo any additional purification. Commercial PW, titanium (IV) isopropoxide (TTIP) ($TiC_{12}H_{28}O_{14}$, 97.0% from Aldrich), and ethanol (EtOH) absolute anhydrous (C_2H_5OH from CARLO ERBA Reagents S.A.S.) are all relevant in this regard.

3.2 Amorphous TiO_2 nanoparticles Synthesization

The synthesization of a-TiO_2 NPs was achieved by hydrolysis of TTIP in the presence of EtOH. The synthesization technique used has been described in [12, 13]. According to the conventional procedure, 97 mL of EtOH and 3 mL of distilled water were combined to create a solution of ethanol and water. 3.7 mL of TTIP was then progressively added to the solution. The resulting mixture was then matured in a typical environment for 36 hours after being stirred with a magnetic stirrer for an hour at room temperature (RT). The resulting solution was then inserted into a porcelain crucible and heated to 100 ^oC for 8 hours to produce a fine white powder.

3.3 Preparation of PW/a-TiO_2 nanocomposites

PW/a-TiO_2 NCs were produced by mixing melted PW with a-TiO_2 NPs that were synthesized. This was done by heating a fixed quantity of PW (5 g) for each sample until it melted completely. Then, the required quantity of a-TiO_2 NPs was added to the melted PW. The weight percentages of TiO_2 NPs into PW in this study are 0, 0.05, 0.1, 0.15, 0.2, 0.25, 0.3, and 0.5% corresponding to labeled sample P, P/0.05AT, P/0.1AT, P/0.15AT, P/0.2AT P/0.25AT, P/0.3AT and P/0.5AT, respectively. The solution for each sample was exposure to a magnetic stirrer for one hour at melted temperature to disperse NPs through the melted PW. In order to obtain uniform NPs dispersion, the resultant solution of each sample was exposed to ultrasonic radiation using a high power ultrasonic homogenizer, model UP 400s, at melting temperature of PW for 15 min. **Table (1)** lists the weight percentages that were used along with their matching designations.

3.4 Characterizations and measurements

Using a PANalytical X'Pert PRO MRD X-ray diffractometer and a CuK radiation source at 1,800 W power (45 kV, 40 mA) with a wavelength of (λ = 0.15406 nm) and a diffraction angle (2θ) from 10° to 80° with a 0.02° increment, the microstructure of the prepared a-TiO_2 NPs was examined. The surface morphology of the produced PW/a-TiO_2 NCs as well as-synthesized TiO_2 NPs was examined using a field-emission scanning electron microscope (FE-SEM, Quanta FEJ20). Differential scanning calorimetry (DSC) measurements of PW/a-TiO_2 NCs were carried out using SETARAM DSC131 Evo instrument at temperature domain from RT to 120 ^oC and a constant heating rate of 10 ^oC/min to evaluate some of the thermal parameters, such as latent heat of melting (LH) and melting temperature (Tm). The DSC tests were performed in a dynamic nitrogen (N_2) environment with an autonomously controlled flow rate.

4. Test Results and Discussion

4.1 Microstructure and morphology of NPs

The XRD pattern of the synthetic TiO_2 is shown in **Fig. (1)**. The diffraction pattern lacks any discernible diffraction lines, as shown in **Fig. (1)**. The resulting pattern clearly demonstrates a step-hump that indicates the TiO_2 is amorphous. This result is frequently obtained by hydrolyzing TTIP followed by drying at 100°C, as reported elsewhere [12, 14, 15]. The FE-SEM micrographs of the investigated TiO_2 NPs are shown in **Fig. (2)**. This picture confirms the amorphous nature of the TiO_2 sample by generating spherical-shaped particles of varying sizes in microsize and nanosize. Amorphous TiO_2 typically has particles that are relatively big in size. Regardless, both microparticles and nanoparticles have considerable surface roughness due to the existence of seed nuclei of few nanosize on the particle's surface, as reported for amorphous TiO_2 synthesized by sonochemical hydrolysis [12].

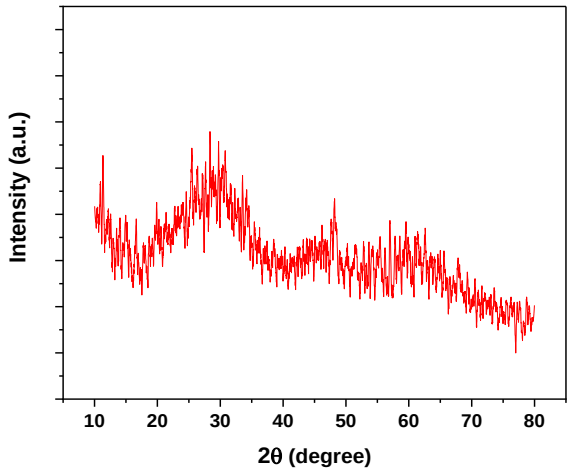

Fig. (1) – XRD pattern of the synthesized TiO_2 NPs

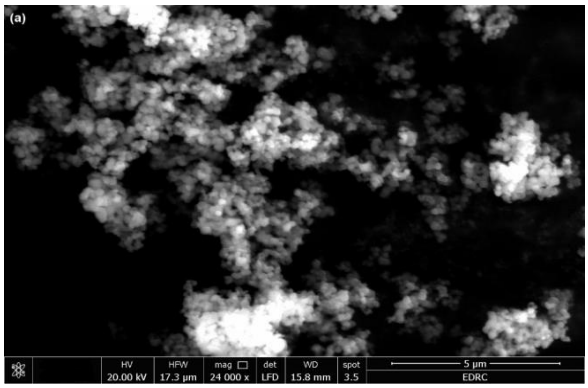

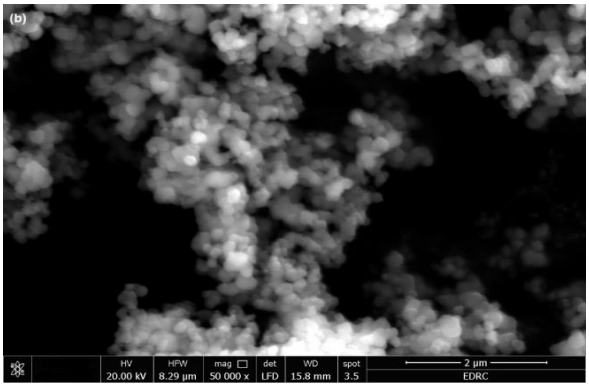

Fig. (2) – FE-SEM micrographs of the investigated TiO_2 nanoparticles: **(a)** micrograph with 24,000x magnification and 5-µm scale; **(b)** micrograph with 50,000x magnification and 2-µm scale

4.2 DSC analysis of the composites

The DSC thermograms of the prepared PW/a-TiO_2 NCs under investigation, which were produced at fixed heat rate of 10 °C/min, are shown in **Fig. (3)**. Two endothermic peaks that are attributed to solid-solid and solid-liquid transitions are the distinguishing features of the DSC curve for all the NC samples. As evidenced by the polymorph trait in material as a result of transformation from one form of crystalline-solid into another, the solid-solid transition actually occurs by variation in temperature or pressure [16]. The crystalline solid-solid transformations are frequently accompanied by irregular changes in volume, enthalpy, and entropy as a result of altered crystal packing. When compared to variations brought on by solid-liquid transitions, these variances have minor values. Therefore, solid-liquid transitions are crucial for the creation of TES based on PCMs. The estimated characteristic parameters of the researched NCs' solid-liquid transition (melting process) are listed in **Table (1)**. The melting temperature (Tm), latent heat of melting (LH), and heat storage power for 1 g (SP, latent heat rate) are calculated from DSC curves and given in **Table (1).** According to the LH values, all of the NCs tested have greater latent heat capacities than pure PW. This shows that PW and a-TiO_2 NPs interacted successfully across the concentration range investigated. Furthermore, due of the altered coordination geometry of their structure in regard to surface defect sites, the latent heat capacity of NCs may be increased [17]. The maximum value of the LH, 197.2 Jg^{-1}, was achieved for 0.15 weight percent loading of a-TiO_2 NPs, an improvement of 19.1% over that for pure PW. According to J Wang et al. [8], introducing 0.7 weight percent TiO_2 NPs on PW resulted in a 14% increase in latent heat capacity.

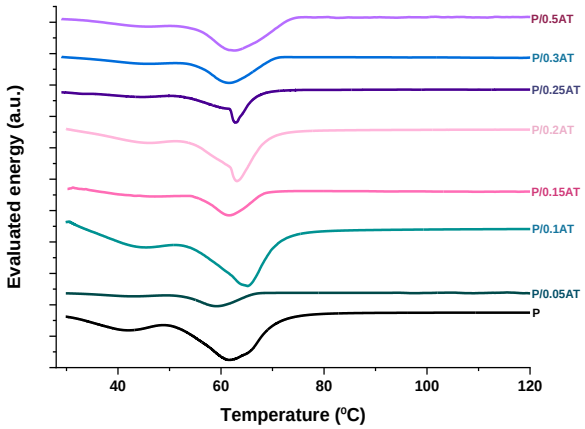

Fig. (3) – DSC curves for the investigated PW/a-TiO_2 NCs

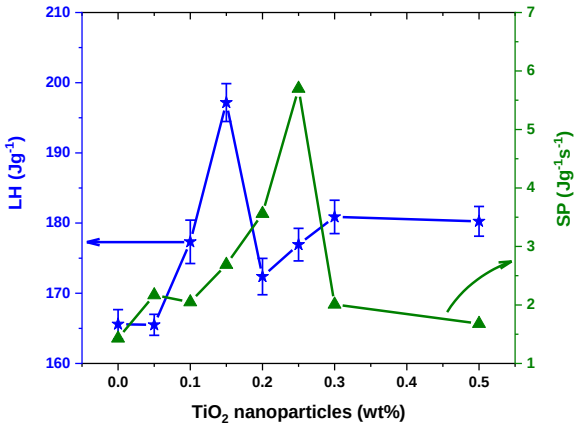

Fig. (4) – The dependency of LH and SP on a-TiO_2 NP concentrations

As seen from **Table (1)**, the NC sample loaded with 0.25 wt% of TiO_2 NP has the greatest value of SP, 5.70 $Jg^{-1}s^{-1}$, an improvement of 298.6% above the estimate for pure PW. **Fig. (4)** displays the dependency of LH and SP on a-TiO_2 NP concentrations. Such a Figure indicates the non-monotonic change of LH and SP with TiO_2 NP content. SP value was improved with TiO_2 content up to 0.25 wt% and then decreased for further contents. While LH was enhanced with TiO_2 content up to 0.15 wt% content and then decreased for further contents. In particular, higher LH levels were obtained for the NCs with various NP concentrations (P/0.15AT, P/0.3AT, and P/0.5AT) than for the P/0.25AT NC. For SP values for these samples, the outcome was the opposite, which can be attributed to the impact of viscosity change on spontaneous convective heat transfer. It should be highlighted that the changing in dynamic behavior of the material depends on the loading of NPs into PW. In particular, the insertion of NPs into PCM causes an increase in the thermal conductivity of PCM along with a clear rise in melt viscosity, which reduces the melt's ability to transfer heat by natural convection [18]. The detected restriction in natural convective heat transfer at high NP loading was made up for by a notable increase in thermal conductivity, as demonstrated by SP behavior. The results obtained indicated that P/0.25AT NC presented the highest heat storage power value for 1 g, indicating that this sample had a higher effective heat capacity than the other samples under investigation.

FE-SEM micrographs of NCs loaded with 0.15 wt% amorphous titanium NPs and pure paraffin, are shown in **Fig. (5)** to show the morphological alterations generated by NP insertion. Small bright spots connected to the a-TiO_2 nanoparticle fillers are visible throughout the PW in the micrograph of the P/0.15AT in **Fig. (5b)**. The employed fabricating process for NCs provided a good contact between a-TiO_2 nanoparticle and PW, as seen in the obtained FE-SEM micrograph P/0.15AT, which shows a pretty excellent dispersion

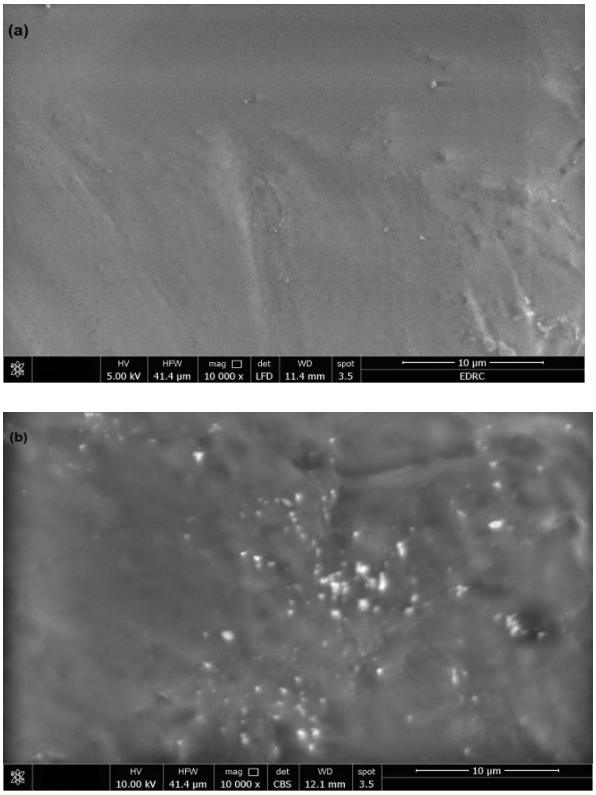

Fig. (5) – FE-SEM micrographs with 10,000x magnification and 10-µm scale for samples: **(a)** P; **(b)** P/0.15AT

Table (1) – Thermal characteristic parameters obtained from DSC measurements for the investigated PW/a-TiO_2 NCs

Sample	TiO_2:PW wt%	T_m/ ºC	L_H/ Jg^{-1}	SP/ $Jg^{-1}s^{-1}$
P	0	60.80	165.6 ± 2.1	1.43
P/0.05AT	0.05	59.28	165.5 ± 1.5	2.17
P/0.1AT	0.1	65.19	177.3 ± 3.1	2.05
P/0.15AT	0.15	61.64	197.2 ± 2.7	2.69
P/0.2AT	0.2	63.13	172.4 ± 2.6	3.56
P/0.25AT	0.25	62.86	176.9 ± 2.3	5.70
P/0.3AT	0.3	61.80	180.9 ± 2.4	2.02
P/0.5AT	0.5	62.83	180.3 ± 2.1	1.68

5. Conclusions

A-TiO_2 NPs loaded onto embedded PW in concentrations up to 0.5 weight percent have been created. The acquired XRD results supported that the synthesized TiO_2 NPs were in the amorphous phase. FE-SEM micrographs have been used to demonstrate and confirm the successful dispersion of a-TiO_2 NPs into PW, indicating a successful interaction between a-TiO_2 NPs and PW. Through the use of non-isothermal measurements, the impact of insertion of a-TiO_2 NPs on the thermal characteristics of PW was examined. The inclusion of a-TiO_2 NPs resulted in a notable improvement in PW's thermal performance. In this regard, an increase in latent heat capacity of 19.1% was achieved for a-TiO_2 NP dose of 0.15 wt%. The thermal storage power (SP) increased significantly for P/0.25AT compared to PW, reaching 298.6%. However, for concentrations more than 0.25 wt%, SP values declined, which may be explained by a restriction in natural convective heat transmission brought on by the rise in melt viscosity. In thermal energy storage (TES) devices, PW/a-TiO_2 nanocomposite is regarded as an appropriate medium.

6. References

[1] S. Zhang, D. Feng, L. Shi, L. Wang, Y. Jin, L. Tian, Z. Li, G. Wang, L. Zhao, Y. Yan "A review of phase change heat transfer in shape-stabilized phase change materials (ss-PCMs) based on porous supports for therma energy storage", Renewable and Sustainable Energy Reviews, Elsevier, vol. 135(C).

[2] R. Agrawal, K.D.P. Singh "A review on productivity enhancement of solar still by application of PCM and nano enhanced PCM", AIP Conf. Proc. 2341 (2021) 5.

[3] K. Pielichowska, K. Pielichowski "Phase change materials for thermal energy storage," Progress in Materials Science, vol. 65, pp. 67-123, 2014.

[4] M. Mofijur, T.M.I. Mahlia, A.S. Silitonga, H.C. Ong, M. Silakhori, M.H. Hasan, N.Putra, S.M. Ashrafur Rahman "Phase change materials (PCM) for solar energy usages and storage: An overview", Energies 12 (16) (2019) 8.

[5] A. Kürklü, A. Özmerzi, S. Bilgin "Thermal performance of a water-phase change material solar collector," Renewable Energy, vol. 26, no. 3, pp. 391-399, 2002.

[6] B. Zalba, J. M. Marín, L. F. Cabeza, H. Mehling "Review on thermal energy storage with phase change: materials, heat transfer analysis and applications," Applied Thermal Engineering, vol. 23, no. 3, pp. 251-283, 2003.

[7] TP. Teng, CC. Yu "Characteristics of phase-change materials containing oxide nano-additives for thermal storage," Nanoscale Research Letters, vol. 7, pp. 611, (2012).

[8] J.-f. Wang, H. Xie, Z. Guo, L. Guan, Y. Li "Improved thermal properties of paraffin wax by the addition of TiO_2 nanoparticles," Applied Thermal Engineering, vol. 73, pp. 1541-1547, 2014.

[9] C. J. Ho, J. Y. Gao "Preparation and thermophysical properties of nanoparticle-in-paraffin emulsion as phase change material," International Communications in Heat and Mass Transfer, vol. 36, no. 5, pp. 467-470, 2009.

[10] D. G. Gunjo, S. R. Jena, P. Mahanta, P. S. Robi "Melting enhancement of a latent heat storage with dispersed Cu, CuO and Al_2O_3 nanoparticles for solar thermal application," Renewable Energy, vol. 121, pp.

652-665, 2018.

[11] B. Prasai, B. Cai, M. K. Underwood, J. P. Lewis, D. A. Drabold "Properties of amorphous and crystalline titanium dioxide from first principles," Journal of Materials Science, vol. 47, 7515–7521 (2012).

[12] S. A. Mansour "Non-isothermal crystallization kinetics of nano-sized amorphous TiO_2 prepared by facile sonochemical hydrolysis route," Ceramics International, vol. 45, no. 2, Part B, pp. 2893-2898, 2019.

[13] F. H. Alkallas, K. M. Elshokrofy, S. A. Mansour "Structural and diffuse reflectance characterization of cobalt-doped titanium dioxide nanostructured powder prepared via facile sonochemical hydrolysis technique," Nanomaterials and Nanotechnology, vol. 9, p. 1847980419847806, 2019.

[14] C. Y. Jimmy, J. Yu, W. Ho, and L. Zhang "Preparation of highly photocatalytic active nano-sized TiO_2 particles via ultrasonic irradiation," Chemical Communications," pp. 1942-1943, 2001.

[15] F. H. Alkallas, T. A. AL-Rebdi, S. A. Mansour "Structural and diffuse reflectance investigation of dysprosium-doped TiO_2 nanopowder synthesized by sonochemical hydrolysis technique," Physica B: Condensed Matter, vol. 603, 2021.

[16] S. Z. D. Cheng "Chapter 2 - Thermodynamics and Kinetics of Phase Transitions," in Phase Transitions in Polymers, S. Z. D. Cheng Ed. Amsterdam: Elsevier, pp. 17-59, 2008.

[17] N. Sahan, H. O. Paksoy "Thermal enhancement of paraffin as a phase change material with nanomagnetite," Solar Energy Materials and Solar Cells, vol. 126, pp. 56-61, 2014.

[18] N. S. Bondareva, M. A. Sheremet "Effect of Nano-Sized Heat Transfer Enhancers on PCM-Based Heat Sink Performance at Various Heat Loads," Nanomaterials, vol. 10, no. 1, 2020.